ELSEVIER

Journal of Alloys and Compounds 466 (2008) 457–462

Journal of ALLOYS AND COMPOUNDS

www.elsevier.com/locate/jallcom

Reaction mechanism and kinetic analysis of the formation of Sr_2SiO_4 via solid-state reaction

Chung-Hsin Lu *, Po-Chi Wu

Electronic and Electro-optical Ceramics Lab, Department of Chemical Engineering, National Taiwan University, Taipei, Taiwan, ROC

Received 7 August 2007; received in revised form 12 November 2007; accepted 16 November 2007
Available online 22 November 2007

Abstract

The kinetics for the formation of Sr_2SiO_4 during solid-state reaction is investigated using an isothermal method. TG/DTA and XRD analysis suggest a direct reaction between $SrCO_3$ and SiO_2 powders. The conversion ratios of the Sr_2SiO_4 starting materials are calculated from the weight loss. Based on the reaction kinetic isothermal analysis, Sr_2SiO_4 formation is corroborated as controlled by the Brounshtein-Ginstling's diffusion-controlled model. The formation process activation energy is estimated to be 139.6 kJ/mol. According to microscopic observations, the microstructures vary drastically at 830 °C, implying a reaction initiation involving reactive $SrCO_3$ and SiO_2. In view of the diffusion controlled mechanism and microstructural observations, a reaction model for the formation of Sr_2SiO_4 has been established.
© 2007 Elsevier B.V. All rights reserved.

Keywords: Sr_2SiO_4; Kinetics; Solid-state; Phosphor

1. Introduction

White light illumination applications have increased in recent years. Traditionally, white light is produced by a phosphor layer coated onto the inner side of lamp tubes under excitation around 280 nm. However, white light has the drawbacks of low power efficiency, reliability and lifetime. In comparison, the light emitting diode (LED) could be considered the next generation light illumination source due to its high reliability and low energy consumption. The first high brightness GaN-based blue light emitting diode prototype was developed in 1993 [1].

To obtain white light through GaN-based LEDs, luminescent materials coated on the top of an LED chip is a promising approach. However, the excitation source provided by blue emitting LEDs (400–490 nm) is different from conventional excitation sources. Consequently, phosphors with different excitation characteristics are required to achieve efficient light conversion. YAG:Ce^{3+} ($Y_3Al_5O_{12}$:Ce^{3+}) with a highly stable structure is a commercially available yellow phosphor used for white LEDs [2–4]. However, it has problems of low color stability with increasing applied current, low color rendering index, and low color reproducibility [5,6]. Another new type of phosphor-Sr_2SiO_4:Eu^{2+} has attracted researchers' attention [7–10]. Sr_2SiO_4 provides the broadband absorption in UV/Blue region due to low symmetry of the crystallographic sites. In addition, the Sr_2SiO_4:Eu^{2+} phosphor has a higher luminous efficiency, CRI and color stability than YAG [10,11], giving rise to a new phosphor approach for white LED applications. Therefore, Sr_2SiO_4 is a suitable host lattice for phosphor applications.

Sr_2SiO_4 powder is usually prepared in a solid-state reaction by heating mixed strontium and silicon salts at elevated temperatures. Although the photoluminescent properties of Sr_2SiO_4 have been explored, the formation mechanism and reaction kinetics have not been studied. Knowledge of the fundamental reaction kinetics and mechanism are important when optimizing the solid-state process for phosphor applications.

In this study, Sr_2SiO_4 powders were prepared via solid-state reaction by heating mixed precursors at elevated temperatures. The purpose of this study is to elucidate the reaction mechanism and reaction kinetics of formation of Sr_2SiO_4 in a solid-state reaction. The precursors were examined using thermal and X-ray diffraction analysis to determine the optimum reaction

* Corresponding author.
E-mail address: chlu@ntu.edu.tw (C.-H. Lu).

0925-8388/$ – see front matter © 2007 Elsevier B.V. All rights reserved.
doi:10.1016/j.jallcom.2007.11.066

range. The isothermal analysis was adopted to understand the reaction mechanism and kinetics. Using the microstructural observations accompanied by the kinetics, a reaction model for the formation of Sr_2SiO_4 via the solid-state reaction is proposed.

2. Experimental

Analytical grade strontium carbonate ($SrCO_3$, Aldrich Chemicals, 99.9%), and silicon dioxide (SiO_2, −325 mesh, Aldrich Chemicals, 99.6%) were mixed in their stoichiometric ratio according to the Sr_2SiO_4 chemical formula. The mixture was ball milled with ethyl alcohol as a dispersing agent and zirconia (ZrO_2) ball for 24 h. The slurry was subsequently dried in a vacuum-rotation dryer.

Differential thermal analysis (DTA) and thermogravimetry analysis (TGA) were applied for tracing the reaction processes. The heating rate was 10 °C/min with alumina powder used as a reference. For isothermal heating experiments, the heating temperatures were set at 700 °C, 750 °C, and 800 °C. The heated samples were soaked after different heating time at the above three temperatures. The phase and purity of the heated powders were examined using the powder X-ray diffraction method with a X-ray diffractometer (MAC Science MXP3). The morphology, grain size, and microstructure of the products were analyzed using a scanning electron microscope (SEM, Hitachi S-800).

3. Results and discussion

3.1. Formation process of Sr_2SiO_4

The powder derived from mixing $SrCO_3$ and SiO_2 was soaked between 600 °C and 1000 °C, at 100 °C intervals. The corresponding XRD patterns are illustrated in Fig. 1. According to the XRD results shown in Fig. 1, it was found that after quenching at 600 °C, no difference was exhibited between the sample and the precursor. This implied that $SrCO_3$ and SiO_2 did not react at below 600 °C. As the firing temperature increased, more Sr_2SiO_4 product was formed, with a corresponding decrease in $SrCO_3$ and SiO_2. When the quenching temperature was raised to 900 °C, the diffraction peaks of $SrCO_3$ and SiO_2 decreased dramatically and nearly all of the major diffraction peaks conformed with the standard powder diffraction profile of Sr_2SiO_4 in the ICDD database, No. 761494 [12]. Sr_2SiO_4 formation was completed when the temperature reached 1000 °C, and no $SrCO_3$ and SiO_2 could be detected. Because no intermediate phase was detected at temperatures ranging from 600 °C to 1000 °C, the Sr_2SiO_4 formation process was confirmed to be a direct reaction between $SrCO_3$ and SiO_2.

Fig. 2 illustrates the DTA/TGA curves for the Sr_2SiO_4 precursors heated at rate of 10 °C/min. The TG-DTA analysis showed two stages of weight loss accompanied by two endothermic peaks. One small endothermic peak at 450 °C in DTA curve, corresponding to the weight loss shown in TG, was due to precursor dehydration. An apparent weight loss occurred at around 700 °C, and no further weight loss was found at temperatures higher than 980 °C. To explain the broad endothermic peak at around 820 °C, the DTA/TG analysis for pure strontium carbonate and silicon dioxide (SiO_2) were also performed. According to our experimental results, the silicon dioxide seemed to be stable in comparison with strontium carbonate in the range of 25 °C to 1000 °C. The results are not shown here. As a result, the endothermic peak at 820 °C shown in Fig. 2 was attributed to reactive strontium carbonate reacting with stable silicon oxide, thereby leading to the formation of Sr_2SiO_4. The total weight loss measured from TG experiment amounted to 24.7%, which was closed to the theoretical weight loss of this reaction. The net equation of the reaction involving $SrCO_3$ and SiO_2 is given in Eq. (1).

$$2SrCO_3 + SiO_2 \rightarrow Sr_2SiO_4 + 2CO_2 \quad (1)$$

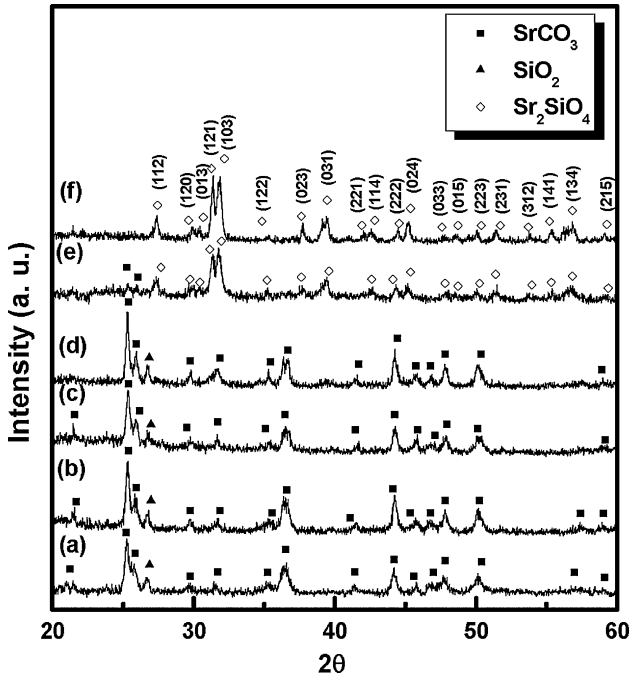

Fig. 1. X-ray diffraction patterns of (a) raw materials of Sr_2SiO_4, and the samples quenched at (b) 600 °C, (c) 700 °C, (d) 800 °C, (e) 900 °C, and (f) 1000 °C.

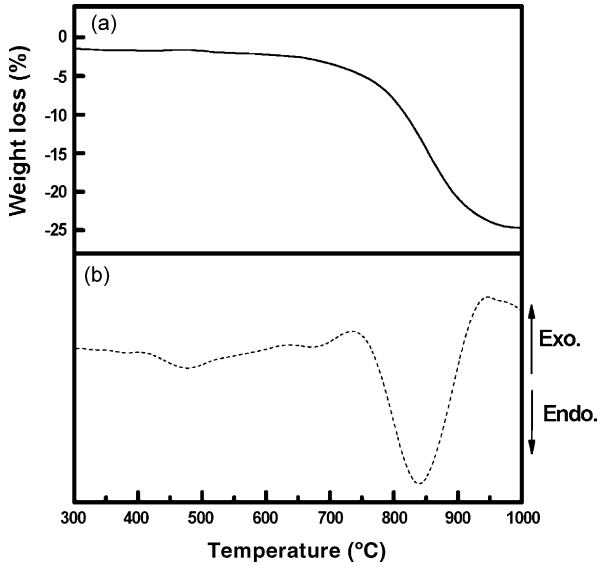

Fig. 2. (a) Differential thermal analysis and (b) thermogravimetry analysis for the starting materials of Sr_2SiO_4 at a heating rate of 10 °C/min.

Table 1
Stoichiometric table for the formation of Sr_2SiO_4

Species	Initially	Change	Remaining
$SrCO_3$	$2X$	$2\alpha X$	$2X(1-\alpha)$
SiO_2	X	αX	$X(1-\alpha)$
Sr_2SiO_4	0	0	αX
CO_2	0	0	$2\alpha X$

X: specific moles. α: fraction converted to Sr_2SiO_4.

3.2. Reaction kinetics analysis

During the reaction indicated in Eq. (1), the conversion ratio of Sr_2SiO_4 can be calculated from the weight loss of the samples. The detailed calculations are described as follows. According to Table 1, the weight before the reaction ($W_{initial}$) is $2XM_{SrCO_3} + XM_{SiO_2}$; the weight after the reaction (W_{final}) is $2X(1-\alpha)M_{SrCO_3} + X(1-\alpha)M_{SiO_2} + aXM_{Sr_2SiO_4}$. Set $\Delta W\%$ as the percentage of weight loss after the quench experiment. Make mass balance as follows:

$$[2XM_{SrCO_3} + XM_{SiO_2}] \cdot \Delta W\% = W_{initial} - W_{final} = 2\alpha XM_{SrCO_3} + \alpha XM_{SiO_2} - \alpha XM_{Sr_2SiO_4}. \quad (2)$$

Rearranging Eq. (2) gives

$$\alpha = \frac{(2M_{SrCO_3} + M_{SiO_2}) \cdot \Delta W\%}{(2M_{SrCO_3} + M_{SiO_2} - M_{Sr_2SiO_4})} = \frac{\Delta W\%}{24.77\%}. \quad (3)$$

where X is specific moles, M_{SrCO_3} is the molecular weight of $SrCO_3$, M_{SiO_2} is the molecular weight of SiO_2, $M_{Sr_2SiO_4}$ is the molecular weight of Sr_2SiO_4, and α is the fraction converted to Sr_2SiO_4. Take the dehydration of precursors into consideration; the weight loss was 0.92% in TG experiment, hence, the exact conversion of the reaction is revised as

$$\alpha = \frac{\Delta W\% - 0.92\%}{24.77\%}. \quad (4)$$

As deduced from Figs. 1 and 2, for the reaction to proceed, the temperature should be higher than 700 °C. Therefore, the reaction temperatures were chosen at 700 °C, 750 °C and 800 °C, respectively. The mixed Sr_2SiO_4 precursors were isothermally heated at these temperatures for various periods of time and then quenched to room temperature. The weight difference ΔW of each specimen before and after the heating process was recorded. The conversion ratio of Sr_2SiO_4 formation under each heating condition was calculated by Eq. (4). Fig. 3 shows the relation between the conversion ratios and reaction conditions. At 700 °C and 750 °C, the conversion ratio monotonously rose with reaction time. The reaction was nearly completed at 800 °C after 60 min. In addition, it was noted that for the same reaction period, the conversion increased with a rise in the heating temperature. Heating specimens at 700 °C for 120 min increased conversion ratio to about 71%. After reacting for 120 min, the conversion ratios at 750 °C and 800 °C were 95% and 97%, respectively. Fig. 3 indicates that the conversion was enhanced with an increase in reaction temperature and time.

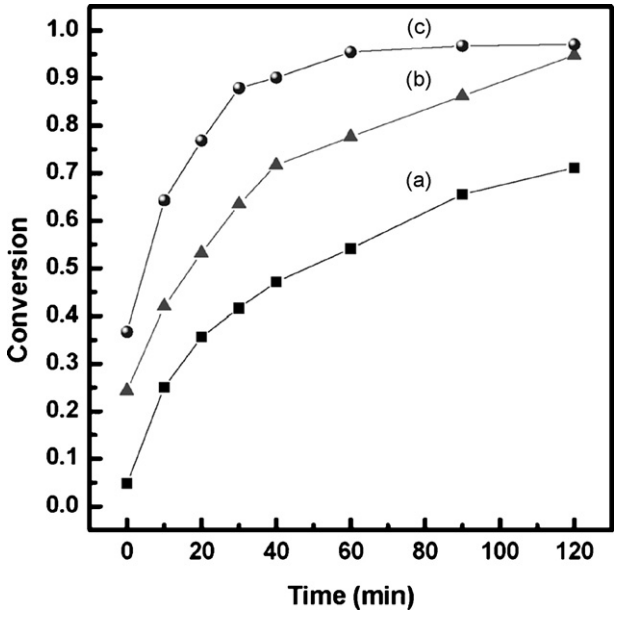

Fig. 3. Conversion ratio of Sr_2SiO_4 versus reaction time.

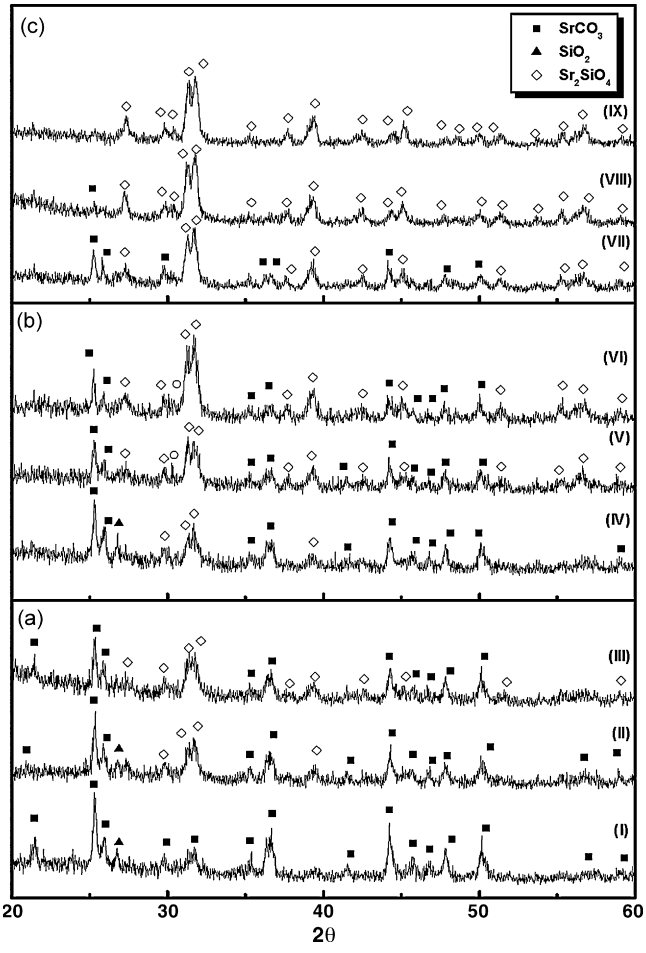

Fig. 4. X-ray diffraction patterns of the starting materials of Sr_2SiO_4 heated at (a) 700 °C for (I) 20 min, (II) 40 min, and (III) 60 min, and (b) 750 °C for (IV) 20 min, (V) 40 min, and (VI) 60 min, and (c) 800 °C for (VII) 20 min, (VIII) 40 min, and (IX) 60 min.

Fig. 4 illustrates XRD patterns of the obtained powders quenched at 700 °C for various reaction time. There was no reaction between $SrCO_3$ and SiO_2 after heating at 700 °C for 20 min, since only the XRD diffraction peaks of $SrCO_3$ and SiO_2 were observed. As the reaction time was prolonged to 40 min, the (1 2 1) and (1 0 3) planes of Sr_2SiO_4 appeared, indicating a small amount of Sr_2SiO_4 began to form. With the increase in reaction time, the intensity of XRD peaks of Sr_2SiO_4 increased rapidly; whereas the intensities of the peaks of $SrCO_3$ and SiO_2 decreased correspondingly. The XRD results for the samples heated at 750 °C and 800 °C are also observed in Fig. 4. As the heating temperature was increased, the diffraction peaks of Sr_2SiO_4 were found at less reaction time and those peaks of $SrCO_3$ and SiO_2 diminished after heating for 40 min at 800 °C.

To analyze the Sr_2SiO_4 reaction kinetics, the Hancock and Sharps' method based on the Johnson-Mehl-Avrami equation was adopted [13,14]. The Johnson-Mehl-Avrami equation is presumed as:

$$\alpha = 1 - \exp(-rt^m) \tag{5}$$

where r is the reaction rate, t is the reaction time, and m is a constant which will vary with the system geometry. With proper linearization processes, Eq. (5) can be written as:

$$\ln[-\ln(1-\alpha)] = \ln(r) + m\ln(t) \tag{6}$$

According to the m values in Eq. (6), the solid-state reactions can be divided into three groups: a diffusion mechanism for $m = 0.54$–0.62, a first-order or phase boundary mechanism for $m = 1.0$–1.24, and a nucleation or growth mechanism for $m = 2.0$–3.0 [15]. By substituting the conversion ratio data from 0 min to 60 min at all three temperatures in Fig. 3 into Eq. (6), one can make a plot of the regression lines of Eq. (6), as shown in Fig. 5. The m values at 700 °C, 750 °C, and 800 °C were estimated to be 0.578, 0.594, and 0.577, respectively. They were

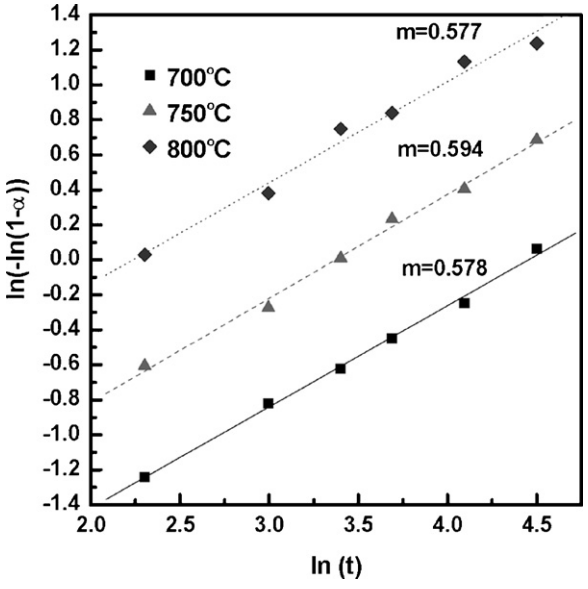

Fig. 5. Plot of $\ln((-\ln(1-\alpha))$ versus $\ln(t)$ for the Sr_2SiO_4 reaction process.

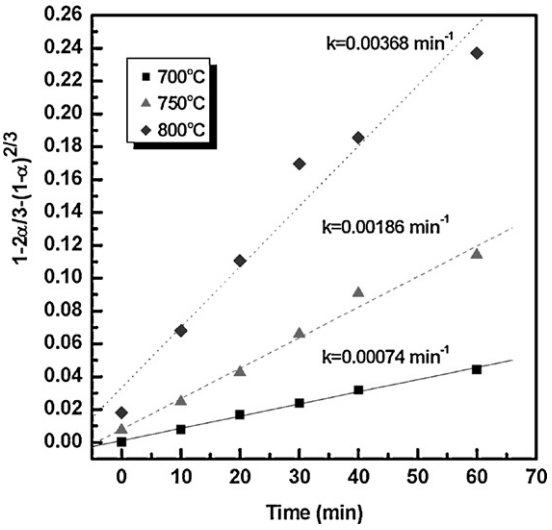

Fig. 6. Plot of $1 - 2\alpha/3 - (1-\alpha)^{2/3}$ versus reaction time for the formation of Sr_2SiO_4.

very close to each other, suggesting the reactions occurred in the studied temperature range were guided by a single reaction mechanism. Comparing the m values with the reaction mechanisms collected by Hancock et al., it is reasonable to conclude that the formation mechanism of Sr_2SiO_4 is a three-dimensional diffusion controlled process. Therefore, the relation between the conversion factor and reaction time for this mechanism can be expressed by the Brounshtein-Ginstling model [16]:

$$1 - 2\alpha/3 - (1-\alpha)^{2/3} = kt \tag{7}$$

where k is the reaction rate constant. By substituting α into Eq. (7) and plotting conversion ratio against reaction time gave the reaction rate at specific temperatures from its slope. From Fig. 6, it can be observed that the values of reaction rate constant k at 700 °C, 750 °C, and 800 °C were 0.00074 min^{-1}, 0.00186 min^{-1}, and 0.00368 min^{-1}, respectively. The activation energy of the reaction was estimated by the Arrhenius equation:

$$k = k_0 \exp\left(\frac{-E}{RT}\right), \tag{8}$$

where E is the activation energy, R is the gas constant, and T is the absolute temperature. Fig. 7 illustrates the plot of $\ln(k)$ versus $1/T$ for Ginstling-Brounshtein model. From the slope of the line in Fig. 7, the activation energy for Sr_2SiO_4 formation was calculated to be 139.6 kJ/mol. These results were similar to the other ceramic reactions [17,18].

3.3. Microstructural observation and reaction model

The surface microstructures of the specimens are shown in Fig. 8. After ball milling for 24 h, the mixtures appeared to be uniform with grain size around 150 nm as shown in Fig. 8(a). When the specimen heated at 800 °C were quenched instantly (Fig. 8b), increase in the grain size of starting materials was observed. Fig. 8(c) shows the sample quenched at 830 °C, reveal-

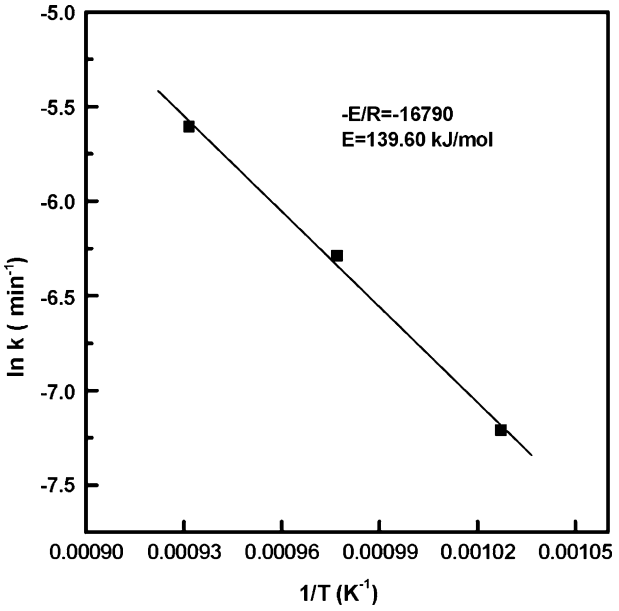

Fig. 7. Plot of ln(k) versus 1/T for the formation of Sr_2SiO_4.

ing drastically varied microstructures having many small islands (∼20 nm) dispersed on the surface of the grains. This suggested that the reactive strontium carbonate decomposed and reacted instantly with the SiO_2 solid particles. When the specimens were quenched at 870 °C (Fig. 8d), the number of islands decreased and the grain growth occurred in the sample, providing evidence of the diffusion process. In addition, from XRD analysis, the crystal structure of these grains was found to primarily consist of Sr_2SiO_4.

In view of the three-dimensional diffusion controlled mechanism with TG/DTA, XRD and SEM results, a microscopic reaction model is proposed and illustrated in Fig. 9. Before the reaction involving $SrCO_3$ and SiO_2, no intermediate product was detected in the samples. As the calcination temperature was increased, $SrCO_3$ reacted with SiO_2 to form the shell of Sr_2SiO_4 on the surface, accompanied by release of carbon dioxide during the reaction. With increasing calcination time, reactive $SrCO_3$ diffused into the core of SiO_2 to thicken the Sr_2SiO_4 shell. The diffusion process was completed with the exhaust of raw materials. Eventually, the pure phase of Sr_2SiO_4 was formed in the samples.

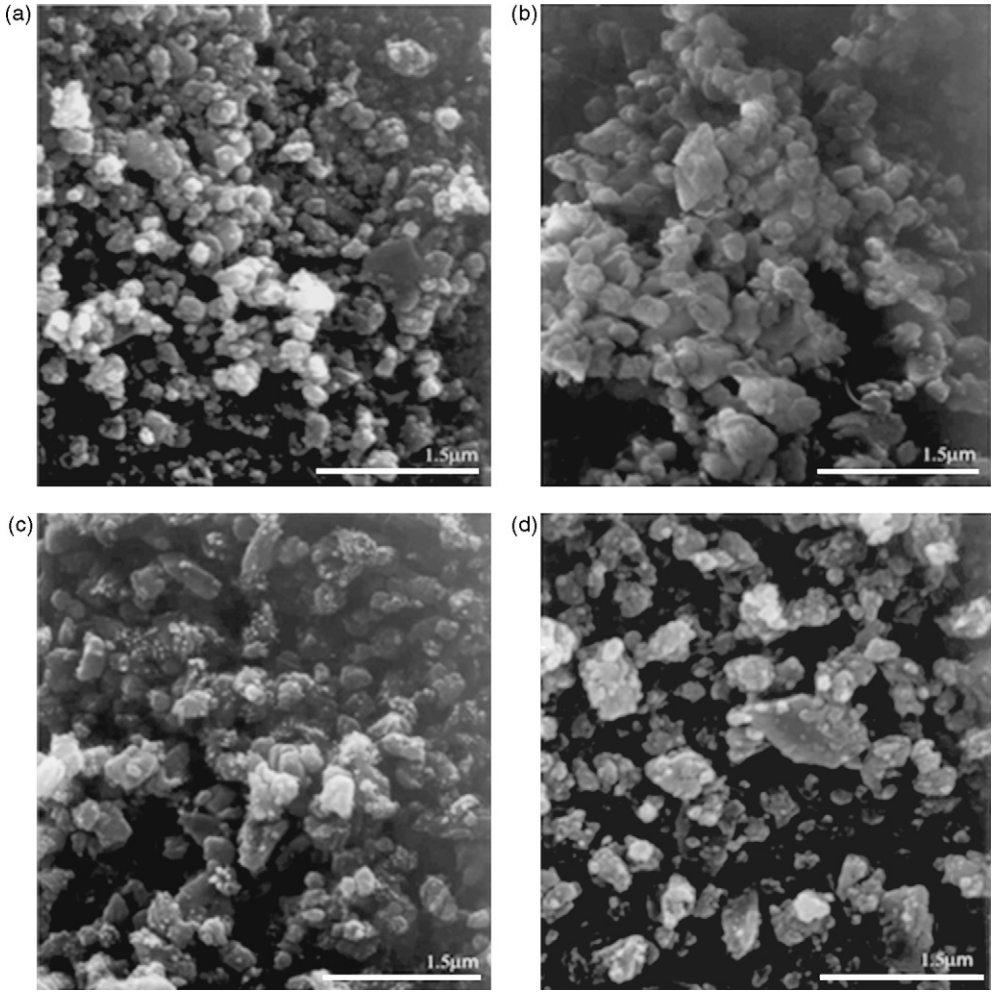

Fig. 8. Scanning electron micrographs of the starting materials of (a) Sr_2SiO_4, and the samples heated at (b) 800 °C, (c) 830 °C, and (d) 870 °C.

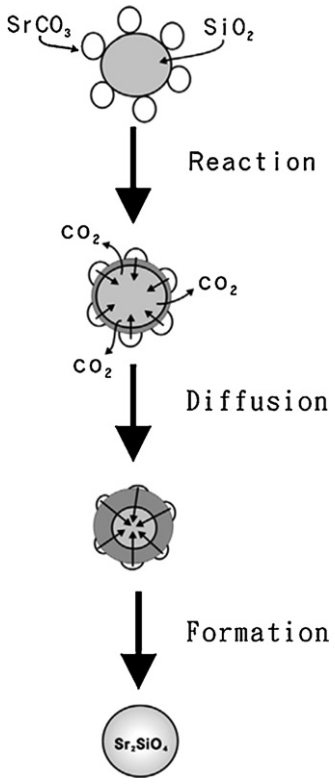

Fig. 9. A microscopic reaction model of Sr_2SiO_4.

4. Conclusions

The reaction mechanism and kinetic analysis for the formation of Sr_2SiO_4 are investigated in this study. The process of formation of Sr_2SiO_4 is assumed to be a direct reaction between $SrCO_3$ and SiO_2 via the TG/DTA and XRD analysis. The conversion of Sr_2SiO_4 from the starting materials increases with an increase in the heating temperature and heating time. For the ceramic reaction involving $SrCO_3$ and SiO_2, the three-dimensional solid-state reaction model is considered. The formation of Sr_2SiO_4 is confirmed to be governed by a diffusion controlled mechanism via reaction kinetic isothermal analysis. According to the Brounshtein-Ginstling model, the activation energy for the formation of Sr_2SiO_4 is calculated to be 139.6 kJ/mol. A microscopic reaction model was also proposed to describe the formation of Sr_2SiO_4, which is a promising phosphor host for use in white light emitting diodes.

References

[1] S. Nakamura, T. Mukai, M. Senoh, Appl. Phys. Lett. 64 (1994) 1687–1689.
[2] Z. Yang, X. Li, Y. Yang, X. Li, J. Lumin. 122/123 (2007) 707–709.
[3] T. Tamura, T. Setomoto, T. Taguchi, J. Lumin. 87/89 (2000) 1180–1182.
[4] D. Jia, Y. Wang, X. Guo, K. Li, Y.K. Zou, W. Jia, J. Electrochem. Soc. 154 (2007) J1–J4.
[5] J.S. Kim, P.E. Jeon, J.C. Choi, H.L. Park, Appl. Phys. Lett. 84 (2004) 2931–2933.
[6] H. Zhang, T. Horikawa, H. Hanzawa, A. Hamaguchi, K.I. Machida, J. Electrochem. Soc. 154 (2007) J59–J61.
[7] G. Blasse, P.E. Wanmaker, J. Vrugt, Philips Res. Rep. 23 (1968) 189–200.
[8] J.S. Yoo, S.H. Kim, W.T. Yoo, G.Y. Hong, K.P. Kim, J. Rowland, P.H. Holloway, J. Electrochem. Soc. 152 (2005) G382–G385.
[9] A. Nag, T.R.N. Kutty, J. Mater. Chem. 14 (2004) 1598–1604.
[10] J.K. Park, M.A. Lim, C.H. Kim, H.D. Park, J.T. Park, S.Y. Choi, Appl. Phys. Lett. 82 (2003) 683–685.
[11] J.S. Kim, J.Y. Kang, P.E. Jeon, J.C. Choi, H.L. Park, T.W. Kim, Jpn. J. Appl. Phys. 43 (2004) 989–992.
[12] M. Catti, G. Gazzoni, G. Ivaldi, G. Zanini, Acta Cryst. B39 (1983) 674–679.
[13] J.D. Hancock, J.H. Sharp, J. Am. Ceram. Soc. 55 (1972) 74–77.
[14] W.A. Johnson, R.F. Mehl, Trans. AIME 135 (1939) 416.
[15] K.W. SEO, J.K. OH, J. Ceram. Soc. Jpn. 108 (2000) 691–696.
[16] A.M. Ginstling, B.L. Brounshtein, J. Appl. Chem. USSR 23 (1950) 1327–1338.
[17] C.H. Lu, C.C. Tsai, J. Mater. Res. 11 (1996) 1219–1227.
[18] C.H. Lu, W.T. Hsu, J.T. Lee, J. Mater. Res. 19 (2004) 2956–2963.